Dislocation Dynamics and Crack Tip Plasticity at the Brittle–Ductile Transition

P. B. HIRSCH, S. G. ROBERTS, J. SAMUELS and P. D. WARREN

Department of Metallurgy and Science of Materials, University of Oxford, Parks Road, Oxford OX1 3PH, UK

ABSTRACT

Recent experiments on the brittle-ductile transition (BDT) of precracked specimens of Si show that the transition is sharp, with a sudden rise in stress intensity factor above the normal low temperature K_{Ic}, and that the strain rate dependence of the transition temperature, T_c, is controlled by dislocation velocity. Etch pit observations show that dislocation generation from the crack tip begins at K just below K_{Ic}, from a small number of sources around the crack tip. The dynamics of plastic relaxation has been simulated on a model in which a small number of crack-tip sources operate and shield the crack. The criterion for failure is that the local stress intensity factor (including dislocation shielding) $K_e=K_{Ic}$. The model predicts cleavage after some plasticity, and that a sharp transition is obtained only if crack-tip sources are nucleated at $K=K_o$ just below K_{Ic}, and if these sources operate at $K=K_N<<K_o$. A mechanism for the formation of crack-tip sources by the movement of existing dislocations to and interaction with the crack tip is proposed. The model predicts a dependence of T_c and of the shape of the BDT on the existing dislocation distribution, and this has been confirmed by experiment. Quantitative agreement is obtained between observed and calculated values of T_c, and its strain rate dependence. The general implications of this work on the conditions for cleavage after plastic flow, and on the role of existing dislocations on the BDT are discussed.

KEYWORDS

Fracture; dislocations; silicon; brittle; ductile.

1. INTRODUCTION

This paper addresses some of the fundamental questions relating to the brittle-ductile transition (BDT) of intrinsically brittle materials containing sharp precracks. At the BDT, plastic relaxation processes (promoted by the high stresses around the crack tip) blunt and shield the cracks, making crack propagation more difficult, resulting in an increase in the fracture stress. Plastic relaxation can occur by the nucleation of dislocation loops at the crack tips by the Rice-Thomson (1974) mechanism, or

by the activation of existing dislocation sources in the material. We shall discuss the relative roles played by these two types of mechanisms.

The brittle-ductile transition temperature (T_c) depends on strain rate. In the case of precracked single crystals of silicon the activation energy controlling T_c is that for dislocation velocity (St.John, 1975; Hirsch *et al.*, 1987, 1988; Brede and Haasen, 1988). To understand the reason for this behaviour a computer model simulating the dynamics of dislocation generation at crack tips has been developed and the predictions of this model are compared with experiment.

2. EXPERIMENTAL APPROACH

We have used precracked single crystals of pure, 'dislocation-free' Si as suitable models for experiments on the fundamentals of the BDT. The stress and temperature dependence of dislocation velocity, in silicon, are well established. The dislocation velocity v can be written

$$v = A\tau^m \exp -U/kT = \tau^m v_o \qquad (1)$$

where U is the activation energy controlling dislocation velocity, τ is the resolved shear stress, m (~1) varies only slowly in the relevant temperature regime (George and Champier, 1979), A is a constant, k the Boltzmann constant, T the temperature, and v_o is the temperature dependent part of the velocity expression. The activation energy depends on doping. Mechanical tests have been carried out using four-point bending of precracked bar-shaped specimens. The fracture plane was a (111) plane, a natural cleavage plane in Si. The sharp precrack was introduced by Knoop indentation at room temperature. Crack depths of 13μm and 37μm were used. This technique also leaves a plastic zone in the region of the indentation; the residual stress was relaxed by annealing the crystals at 800°C in vacuum. Cook and Lawn (1983) have shown that if residual stresses are present, there would be a period of stable crack growth on loading before catastrophic failure occurred. Examination after fracture of the cracks showed no signs of stable crack growth, suggesting that the annealing treatment had removed most of the residual stresses. Dislocation distributions around the crack tip were revealed by using the "Secco" etch (Secco d'Aragona, 1972) on the fracture surfaces. Specimens fractured at room temperature using the above preparation treatment showed no etch pits around the original precrack front.

3. EXPERIMENTAL RESULTS

Figure 1(a) shows curves of applied load against cross-head deflection at a particular strain rate for specimens tested just below (A), at T_c (B), and above T_c (C). At the BDT the specimen fails by cleavage at a higher stress than that below the BDT, but any plastic contribution to the load/deflection curve is not measurable. Above the BDT the whole specimen deforms plastically and does not fracture. Figure 1(b) shows fracture stress against temperature for a given strain rate, for intrinsic Si. The transition is extremely sharp. The range of temperatures from the highest at which a specimen fractures in a completely brittle manner to the lowest at which a specimen deforms plastically is typically about 10°C.

The transition temperature T_c increases by about 100°C when the strain-rate is increased tenfold. Figure 2 shows the results of tests carried out at different strain rates, for intrinsic and n-type material. The precrack depth is 13μm in all experiments except for point C, where the crack depth

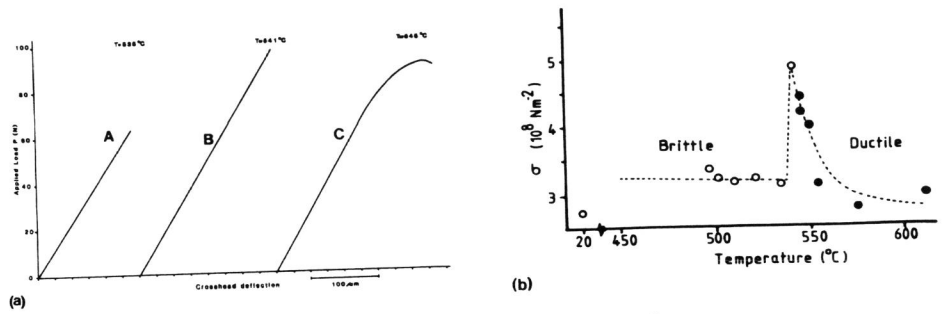

Fig. 1(a) Load-displacement curves for specimens tested just below (A), at (B) and just above (C) the brittle-ductile transition temperature.
(b) Failure stress vs. temperature for intrinsic silicon specimens tested at the minimum strain rate.

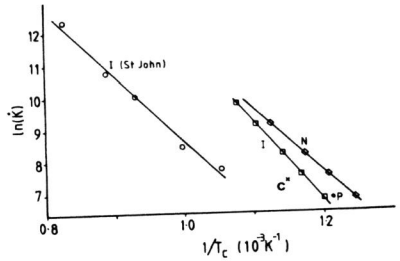

Fig.2 Plots of $\ln(\dot{K})$ versus $1/T_c$ for intrinsic (I) and n-type (N) Si, for the Oxford experiments, and also for St.John's experiments on intrinsic material.

is 37μm. The strain rate is expressed in terms of rate of increase of stress intensity factor, $\dot{K}$, using the expression of Newman and Raju (1981) for a semicircular crack. Figure 2 shows that $\dot{K} \propto \exp -U_e/kT_c$, where U_e is the experimental activation energy. Table 1 compares these activation energies with those for dislocation velocity for similar material. The agreement is within experimental error for both intrinsic and n-type material. This confirms the original suggestion of St.John (1975) that the activation energy controlling the strain-rate dependence of T_c is that for dislocation velocity. It follows from eqn.(1) that, at T_c

$$\dot{K} \propto v_o \qquad (2)$$

Table 1. Activation energies

Experiment	Activation energy	
	Intrinsic Si (2×10^{13} Pcm^{-3})	n-type Si (2×10^{18} Pcm^{-3})
BDT (this work)	2.1±0.1eV	1.6±0.1eV
BDT (St.John, 1975)	1.9eV	-
Disln. velocity (George & Champier, 1979)	2.2eV	1.7eV
Disln. velocity (Imai & Sumino, 1983)*	2.3eV	1.7eV

(* doping levels used were 2×10^{12} Bcm^{-3} and 6.2×10^{18} Pcm^{-3})

Figure 2 also shows St.John's original data for intrinsic Si, obtained using a tapered double cantilever technique. The activation energy is close to that for dislocation velocity for intrinsic material (see Table 1), but there is a considerable shift in T_c to higher values compared with those from the Oxford experiments. Typically the shift is ~100°C for comparable slow strain-rates. Point C obtained for a larger crack-depth (37μm) in intrinsic material does not fall on the line for intrinsic material with the standard 13μm crack depth. This shift to higher temperatures for a larger crack size is significant and will be discussed later.

4. ETCH PITTING STUDIES OF DISLOCATION DISTRIBUTION

Specimens which fractured at test temperatures up to only a few degrees below T_c show no significant dislocation activity. Figure 3(a) shows an etched fracture surface from a specimen tested only 1°C below T_c. Short

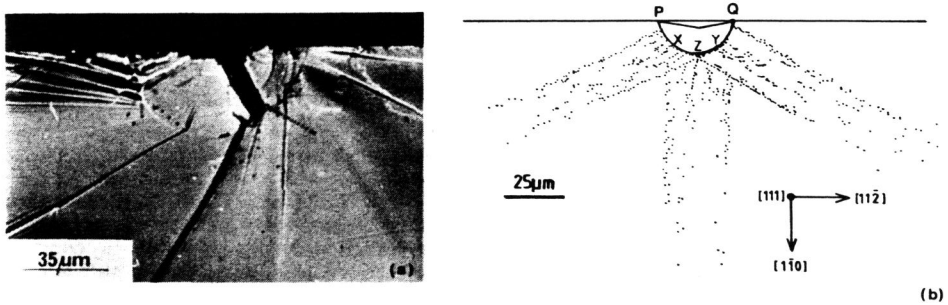

Fig. 3(a) Etched fracture plane of a specimen tested only 1°C below T_c.
(b) Tracing of etched fracture face of a 'transition' specimen; long rays of dislocations emanate from the crack front, mostly from the positions (X,Y,P,Q) where the tangent to the crack front lies in a slip plane.

trains of dislocations apparently coming from the crack profile can be seen, but the amount of dislocation activity is very small. Specimens deformed above T_c in the ductile region, up to the yield stress, show extensive slip over the whole specimen.

However, at the transition temperature, when the specimen fractures at a considerably higher stress than in the low temperature brittle region (see Fig. 1(b)), the etched fracture face shows trains of dislocations along the <110> directions, emanating from the precursor crack. Figure 3(b) shows a tracing of an optical micrograph of such a specimen which failed at $K=1.6$ MPam$^{\frac{1}{2}}$. Trains of dislocations extend about 100μm into the specimen, each containing 80-100 dislocations, approximately in the form of an inverted pile-up. The prominent rows of dislocations appear to come from points where the {111} planes inclined to the cleavage plane are tangential to the crack front. The fracture surface showed no evidence for stable crack extension before fracture.

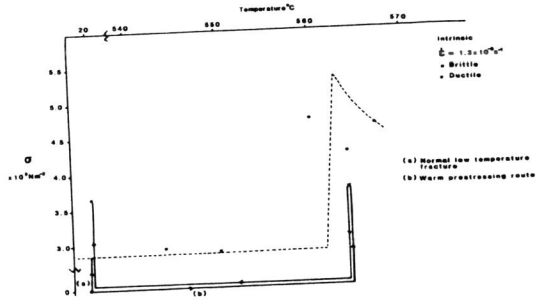

Fig. 4 Warm prestressing in silicon, with 13μm deep precracks. Loading at room temperature (path (a)) leads to fracture at the normal K_{Ic}. Prestressing above T_c (path (b)) increases the room temperature fracture stress.

Tests were carried out in which specimens were deformed just above T_c to a stress about 1.3 times the low temperature fracture stress, unloaded, cooled to room temperature and reloaded to fracture. Figure 4 shows an example; the fracture stress at low temperature is about the same as the stress to which the specimen was loaded at the high temperature. This is the "warm prestressing" effect well known for steels. The etched fracture surface shows etch pit arrays similar to those in Fig. 3(b). In this experiment the dislocations observed are those generated during loading at the high temperature, which are "frozen in" on cooling to room temperature. The similarity between this etch pit distribution and that in a specimen fractured at a similar stress at T_c is strong evidence that no significant plasticity occurs after the crack has become unstable at T_c.

The value of K at which dislocations begin to be emitted at T_c was determined by stressing the specimens at T_c to values of $K<K_{Ic}$, and then fracturing and etching them at room temperature. These tests show that significant dislocation activity at the crack tip, in a constant strain-rate test, begins only at a value of K very close to K_{Ic} ($\sim0.9K_{Ic}<K<K_{Ic}$).

5. A DYNAMIC CRACK TIP SHIELDING MODEL FOR THE BDT

The dislocation distributions revealed by etch pitting at T_c (see Fig. 3(b)) suggest that at the BDT a series of dislocation loops is emitted from sources at or close to the points on the curved crack profile where the {111} glide planes are tangent to the crack profile. Detailed stress analyses (see Hirsch *et al.*, 1989) indicate the mechanism by which this might occur. After formation of the source, the screw parts of the dislocation loop cross-slip around the crack profile, causing crack blunting, while the edge parts of the loop move away from the crack and cause shielding. The local stress intensity factor K_e is given by

$$K_e = K - \Sigma K_D \qquad (3)$$

where K is the applied stress intensity factor, and ΣK_D is the shielding effect of the emitted dislocations (Thomson, 1978; Weertman, 1978; Majumdar and Burns, 1981; for review see Thomson, 1986). We have considered only the shielding effect. The justification for this is that in the present experiments the blunting is likely to be due to screw dislocations which will produce a sharply angled crack opening profile. Sinclair (1985) and Paskin *et al.*, (1985) have shown that for cracks with sharp corners the stress singularity is not much weaker than for an infinitely sharp crack. For this reason, and in order to simplify the problem, we have neglected the blunting effect.

When crack propagation occurs entirely by a brittle mechanism, i.e. bond rupture at the tip, without generation of dislocations, as appears to be the case in the present experiments, the local criterion for fracture in pure mode I loading is that

$$K_{Ie} = K_{Ic}. \qquad (4)$$

During a constant strain-rate test in the transition region, as the applied K increases, ΣK_D will increase as the number of emitted dislocations increases, and K_{Ie} may increase depending on the test conditions. T_c is then defined as the lowest temperature (for a given strain-rate) at which $K_{Ie} < K_{Ic}$ for all points on the crack profile, for all values of $K > K_{Ic}$, up to K with an associated stress level at which general yielding occurs.

To make the modelling tractable, some simplifications have been made:

1. Mode I deformation is replaced by Mode III deformation. In Mode I deformation (edge dislocations on planes inclined to the crack plane) the presence of the crack introduces image dislocations; this leads to complicated interactions in two dimensions (see Thomson, 1986). For Mode III deformation, screw dislocations coplanar with the crack are produced, the image dislocations are on the same plane, and the model becomes one dimensional. Although Mode III calculations may not give numerically correct estimates, they will give valuable insight into the factors important in the dynamics of the problem. We have therefore used the fracture criterion

$$K_{IIIe} = K_{Ic}. \qquad (5)$$

2. The curved crack with multiple sources has been replaced by a straight crack with two sources; the Burgers vector of the dislocations is parallel to the crack front. The geometry is shown in Fig.5.

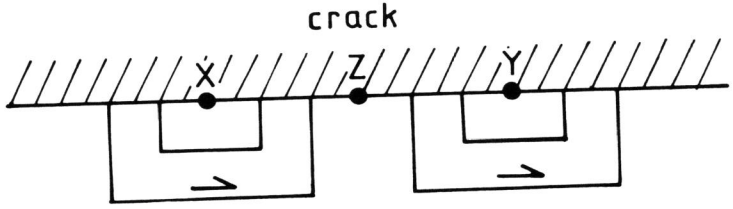

Fig. 5 Simplified model of the crack front and dislocation loops used for the computer simulation. Loops expand from points 'Y' and 'X', eventually to cover point 'Z'.

3. We have assumed that the velocity of the edge components of the loop is the same as for the screws. This implies that the loops are elongated in the screw direction (i.e. the screws are twice as long as the edges). The crack tip and dislocation interaction stresses on the screws have then been calculated assuming them to be straight and parallel, but a line tension term has been included which takes account of the dislocation image stress, and of a curvature effect in an approximate way.

4. The interaction between dislocations from different sources has been neglected.

On these assumptions the stress on any dislocation at x_i is given by

$$\tau_{x_i} = \frac{K}{(2\pi x_i)^{\frac{1}{2}}} - \frac{\alpha\mu b}{x_i} + \frac{\mu b}{2\pi} \sum_{j\neq i} \left(\frac{x_j}{x_i}\right)^{\frac{1}{2}} \frac{1}{(x_i - x_j)} \qquad (6)$$

where x_i is the position of the i^{th} dislocation, x_j that of the j^{th} dislocation, α the line tension/image stress parameter which depends on the shape of the loop (taken = 1/4 in most of the calculations). The first term in equation (6) is the crack tip stress, the second the line tension/image stress term, the third the dislocation/dislocation interaction term (see Thomson, 1986).

Using the expression for dislocation velocity (1) and writing

$$\frac{dx_i}{dt} = \dot{K} \frac{dx_i}{dK},$$

we find

$$\left(\frac{\dot{K}}{v_o}\right)^{1/m} \left(\frac{dx_i}{dK}\right)^{1/m} = \frac{K}{(2\pi x_i)^{\frac{1}{2}}} - \frac{\alpha\mu b}{x_i} + \frac{\mu b}{2\pi} \sum_{j\neq i} \left(\frac{x_j}{x_i}\right)^{\frac{1}{2}} \frac{1}{(x_i - x_j)} \qquad (7)$$

For a constant strain-rate test, i.e. $\dot{K}$=constant, we can therefore determine uniquely the positions of the dislocations x_i as a function of K at a given temperature. The local value of the stress intensity factor at the source, K_{es}, is given by

$$K_{es} = K - \Sigma_j \frac{\mu b}{(2\pi x_j)^{\frac{1}{2}}} \qquad (8)$$

We now assume that the dislocation loops at the source can be nucleated and move away from the tip provided the stress at a critical distance x_c from the tip is sufficient to expand the loop. Once nucleated, the back stress from this dislocation shields the source and the stress at x_c drops. As the dislocations move away, the stress at x_c increases again, and when the critical stress is reached another dislocation is emitted, and the cycle repeats. This mechanism leads to a dislocation-free zone (DFZ), observed and discussed by Ohr (1985). Figure 6 shows schematically how the distance moved by individual dislocations, and K and K_{es} vary during a typical calculation. Figure 6(a) shows the boundary of the dislocation-free zone which is found to decrease slowly with increasing numbers of dislocations emitted. Any new dislocation crosses the DFZ rapidly before joining the more slowly moving train.

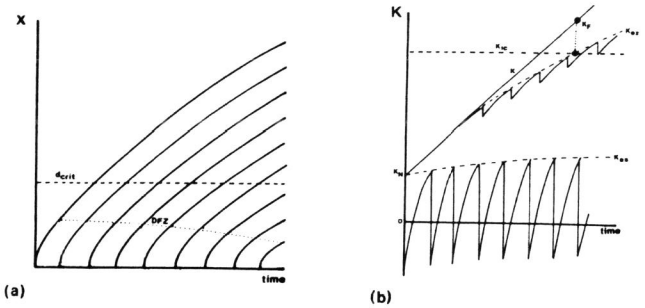

Fig. 6 Schematic illustration of the main features of the computer simulation. (a) Dislocation positions. At d_{crit}, a dislocation can shield point 'Z'. (b) Applied and effective stress intensities at the source (K_{es}) and point 'Z' (K_{ez}).

The condition for nucleation at x_c is

$$\frac{K}{(2\pi x_c)^{\frac{1}{2}}} \geq \frac{\alpha\mu b}{x_c} - \frac{\mu b}{2\pi}\sum_j \left(\frac{x_j}{x_c}\right)^{\frac{1}{2}} \frac{1}{(x_c - x_j)} \qquad (9)$$

The first dislocation is emitted at a critical value of

$$K = K_N = \alpha\mu b(2\pi/x_c)^{\frac{1}{2}} \qquad (10)$$

This value of K_N is indicated in Fig. 6(b). Effective K at the source (K_{es}) rises and falls as each dislocation is emitted. For a given strain rate, the maximum stays close to K_N at high temperatures and increases with time at low temperatures.

We now consider the shielding at the point Z on the crack front. The stress field from any loops from the sources at X and Y which have not yet reached Z might be expected to be antishielding. We have made the simplifying assumption that the point Z on the crack front in Fig. 5 will be shielded only when the dislocation loops have moved past Z. Then the shielding at Z is given by

$$K_{ez} = K - \sum_{j>j_o} \frac{\mu b}{(2\pi x_j)^{\frac{1}{2}}} \qquad (11)$$

summing over all the dislocations which have moved past Z. Thus shielding at Z only starts at a time t_o which depends on the distance XZ. K_{ez} is shown schematically in Fig. 6(b).

Before discussing the detailed computations for Si, certain general conclusions may be drawn from the form of the equations derived so far:

1. The models of mode III fracture discussed by Ohr (1985) and Thomson (1986) distinguish between ductile and brittle regimes according to whether the critical local stress intensity factor for dislocation emission at the crack (K_{ee}) is less or greater than that for brittle fracture (K_{Ic}). The problem with this approach is that if $K_{ee} < K_{Ic}$ dislocation emission will continue to occur and no subsequent cleavage fracture is possible. Sinclair and Finnis (1983) have suggested that cleavage could follow emission if the latter results in a mixed loading situation. (For discussion see Thomson, 1986.) In the present model cleavage is predicted after emission of a certain number of dislocations (see e.g. Fig. 6(b)) for two different reasons. Firstly, as emphasised above, the critical condition for nucleation (equation 9) is that the crack tip **stress** on a dislocation at a certain distance x_c is sufficient to move the dislocation away from the tip against the image/line tension stress and dislocation interactions. Thus x_c corresponds to a critical loop size for nucleation. Equation (9) can be rewritten, using equation (8) to give

$$\frac{K_{es}}{(2\pi x_c)^{\frac{1}{2}}} = \frac{\alpha\mu b}{x_c} + \frac{\mu b}{2\pi}\sum_j \left(\frac{x_c}{x_j}\right)^{\frac{1}{2}} \frac{1}{(x_j - x_c)} \qquad (12)$$

Thus the value of K_{es} at which emission occurs will vary as dislocations are emitted, the change in the K_{es} for emission being controlled by the dislocation interaction term on the r.h.s. of the equation. [When the interaction term is neglected, emission occurs at a constant K_{es} ($\equiv K_{ee}$)]. Essentially the same point has been made by Lin and Thomson (1986) in their discussion of the operation of an external source near the crack tip. For a given $\dot{K}$, below T_c the dislocations move slowly so that the smallest x_j can become comparable with x_c, K_{es} and K_{ez} increase with K, and eventually $K_{ez} > K_{Ic}$ and fracture ensues before further emission occurs. Above T_c the dislocations move rapidly, emission continues throughout the test, and K_{ez} never reaches K_{Ic}. The second reason why cleavage can ensue after a certain number of dislocations has been emitted is the requirement for the dislocations to move a certain distance before they shield the most vulnerable part of the crack (point 'Z').

2. Neglecting the temperature dependence of m, μ, b in the temperature range around the range of values of T_c for different strain-rates, and assuming K_N to be independent of temperature for each value of $(\dot{K}/v_o)$, there is a unique solution from equation (7) of the dislocation distribution as a function of K, and correspondingly a unique variation of K_{es} or K_{ez} as a function of K or time t. There will then be a particular temperature-independent value of $(\dot{K}/v_o)$ for which K_{ez} is just below K_{Ic} for all values of K up to that at which macroscopic plastic flow sets in. Thus, the theory predicts that the values of T_c for different strain-rates satisfy the relation $\dot{K}/v_o(T_c)$ = constant, which is the experimentally observed strain rate dependence of T_c (see eqn. (2)). The key assumption here is that K_N is independent of temperature; it implies that the generation of a new

dislocation is determined only by stress and is not controlled by a thermally activated process. (However, see discussion of a delayed nucleation model in §6).

6. RESULTS OF COMPUTATIONS FOR SI

The program simulates dislocation motion for given 'experimental' conditions of $\dot{K}$ and T. Dislocation nucleation conditions are specified by selection of two of K_N, α and x_c, with the third then determined by equation (10). The actual values of x_c and α used to give a particular value of K_N were not found to influence the results. The calculations begin at $K=K_N$, with one dislocation at $x=x_c$. Values of K_N between $0.2K_{Ic}$ and $0.95K_{Ic}$ were used. With α = 1/4 in equation (10), the former corresponds to $x_c \sim 10.7b$. The dislocation velocity data used were those of George and Champier (1979) for screw dislocations in silicon.

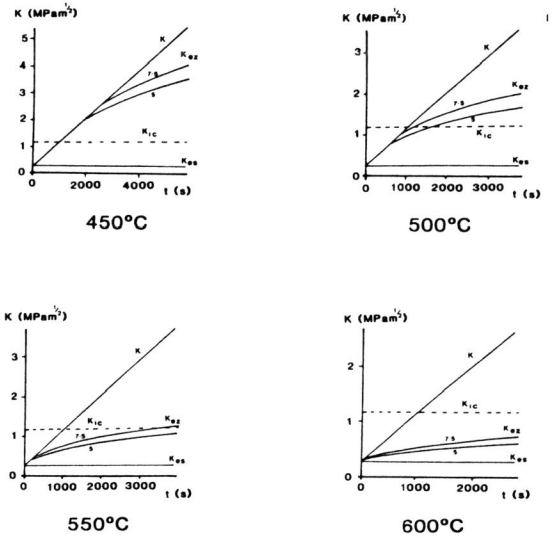

Fig. 7 Computer simulations for $K_N = 0.2K_{Ic}$, for four temperatures close to the BDT showing applied K, K_{es} and K_{ez} for d_{crit} = 5μm and 7.5μm.

Computations have been carried out for various distances $d_{crit} \equiv XZ$, up to 7.5μm, which corresponds to the case for a semicircular crack with radius 13μm, used in most of the experiments. Figure 7 shows a set of curves of K, K_{ez} (for d_{crit} = 5μm and 7.5μm) and K_{es}, for $\dot{K} = 886 Nm^{-3/2}s^{-1}$, and $K_N=0.2 K_{Ic}$, as a function of time at 450°C, 500°C, 550°C and 600°C. It is clear that at 450°C, the expected behaviour would be 'brittle', as K_{ez} diverges from applied K only after K exceeds K_{Ic}. At 500°C, K_{ez} for d_{crit}=7.5μm equals K_{Ic} for values of applied K only just above K_{Ic}. At 550°C, however, K_{ez} does not reach K_{Ic} until $K \gtrsim 3K_{Ic}$; since macroscopic plasticity sets in at $K \sim 2K_{Ic}$, 550°C corresponds to the case when the specimen is expected to be

completely ductile. Thus, $T_c \sim$ 500-550°C for this strain-rate. At 600°C the predicted curves for K_{ez} will not reach K_{Ic} until K is at a level far beyond that corresponding to the macroscopic yielding. Other points to be noted are:

1. Dislocations at any particular time form an inverted pile-up, similar to (but much smaller than) those predicted by static equilibrium calculations (for review see Thomson, 1986) (see Fig. 6(a)).

2. At a given temperature, smaller values of d_{crit} give fracture at larger values of K, implying a smaller T_c; i.e. a size effect is predicted of the type observed experimentally (see Fig. 2).

3. The slopes of the dislocation position versus time curves, are not quite the same for all dislocations at any particular time; i.e. the velocities (and total stresses acting) are smaller for the dislocations at the head of the inverted pile-up, than for those nearer the crack tip. The net stress on any given dislocation decreases slowly with time as it moves away from the crack tip (Fig. 6(a)).

4. In static treatments of the dislocation distribution at a crack tip, the assumption is often made that the dislocations must overcome a constant friction stress τ_f in order to glide away from the crack (Bilby *et al*, 1963; Chang and Ohr, 1981; Ohr, 1985; Thomson, 1986; Lakshaman and Li, 1989). Using reasonable τ_f values for Si (5-10MPa) the length of the static dislocation array is predicted to be very much larger than those predicted from the dynamic models, or seen experimentally. Also, the dislocation arrangements predicted in such treatments differ from those predicted at any particular time from the dynamic treatment, since the total stress acting on a dislocation is found to vary with its position in the moving inverted pile-up.

5. K_{es} is effectively constant except at very low temperatures (≲~300°C), when it increases slowly with time; the emitted dislocations move so slowly that further emissions can occur only when K_{es} increases.

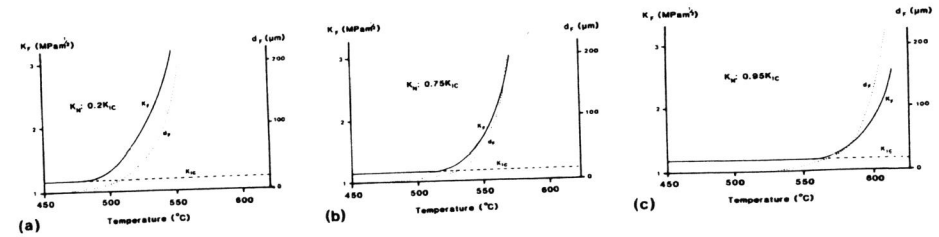

Fig. 8 Predicted variation of BDT with K_N.

Figure 8(a) shows values of K at which fracture occurs, K_F, (i.e. when $K_{ez}=K_{Ic}$) as a function of temperature (at the same $\dot{K}$,K_N as in Fig. 7, and d_{crit}=7.5μm), and the corresponding distances travelled by the leading dislocation in the train, d_F. These curves show clearly that the predicted transition is 'soft', i.e. the fracture stress (proportional to K_F) increases gradually with temperature, and even below T_c(~550°C), say at 500°C, the leading dislocation would have moved large distances and many

dislocations would have been emitted. This behaviour is contrary to that observed; in practice no significant plasticity is detected by etching even a few degrees below T_c, and the curve of K_F versus temperature is very sharp (see Fig. 1(b)). Thus, although the computations predict the correct range for T_c, the sharp nature of the transition is not reproduced. Further calculations have been carried out for higher values of K_N (Figs. 8(b) and (c)). These curves show that the simple model with nucleation beginning and continuing at K_N (even with K_N just less than K_{Ic}) always leads to a soft transition, which is not experimentally observed. Etching experiments (see Fig. 3) suggest that a dislocation nucleation 'event' occurs at a value of applied K just below K_{Ic}. Computations were therefore carried out in which the calculations were started at an applied $K=K_o$, at which dislocations begin to be generated (where $K_N<K_o<K_{Ic}$). This simulates a nucleation event (a possible mechanism for such a delayed nucleation is discussed in §7).

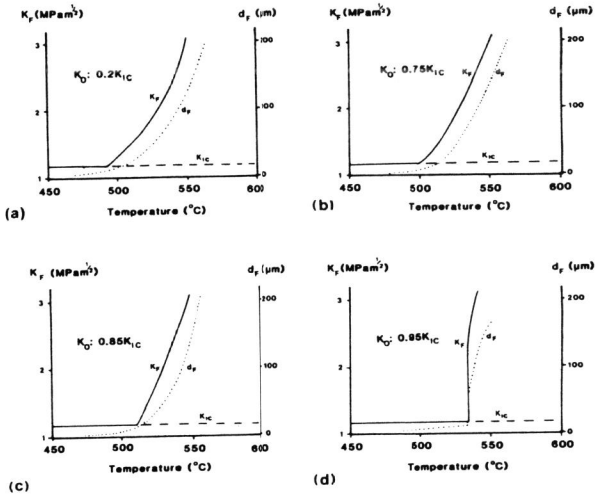

Fig. 9 Predicted variation of BDT with K_o.

Figure 9 shows calculations of K_F and d_F as a function of temperature for four values of K_o, with $K_N=0.2\ K_{Ic}$ and $d_{crit} = 7.5\mu m$. These computations show clearly that a sharp transition is predicted for $K_o \sim 0.95K_{Ic}$, consistent with the experimental observations that no significant dislocation activity occurs at T_c until $\sim 0.9K_{Ic}<K<K_{Ic}$. The value of T_c predicted for this standard strain rate (~535°C) is slightly below the observed T_c (~550°C), but in view of the approximations in the model this can be considered as good agreement. Calculations carried out for $K_o=0.95K_{Ic}$, and various values of K_N, show that for values of $K_N<<K_o$ the form of curves is insensitive to K_N in that a sharp transition occurs, but that as K_N approaches K_o, the transition tends to become soft again. The sharpness of the experimentally observed transition suggests that $K_N<<K_o$, but the exact value of K_N is not known.

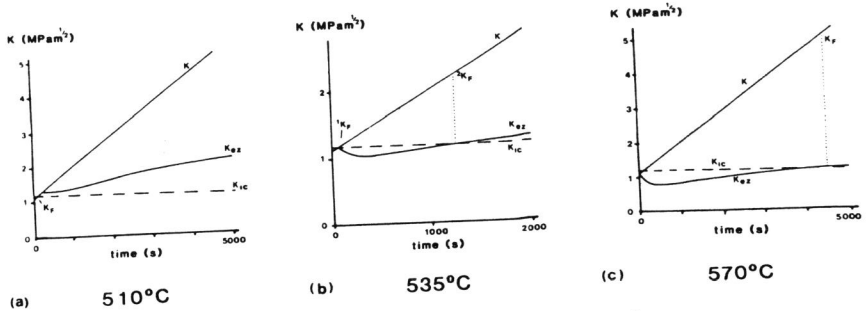

Fig. 10 Characteristics of a sharp brittle-ductile transition. K_{ez} is shown as a function of time for three temperatures: (a) 510°C; brittle. (b) 535°C; transition. (c) 570°C; ductile.

Figure 10 shows calculations of K_{ez} and d_F as a function of time at three temperatures, for $K_N=0.25$ MPam$^{\frac{1}{2}}$, $K_o=0.95K_{Ic}$. At T_c (~535°C) (Fig. 10(b)), K_{ez} drops slightly initially and then increases very gradually with time, predicting fracture at $K_F \simeq 2.1$ MPam$^{\frac{1}{2}}$. This initial drop in K_{ez}, with a longer-term rise, eventually to reach K_{Ic}, is the reason for the steplike sharp transitions in Fig. 9(d). At higher temperatures $>T_c$ (Fig. 10(c)), the drop in K_{ez} is greater and K_{ez} reaches K_{Ic} only after very long times, when applied K is very high (corresponding to stresses above the overall yield stress). At 510°C the behaviour is totally brittle, in that dislocations do not pass Z before K reaches K_{Ic} (Fig. 10(a)). Note that an increase in temperature from just below to just above 535°C will produce a jump in K_F from ^1K_F ($=K_{Ic}$) to ^2K_F.

The curves in Fig. 10 can also be used to make estimates of the distance travelled by the dislocations and of their numbers when fracture occurs in the transition region, or when the specimen is unloaded before fracture occurs. Fig. 3(b) suggests that for a specimen fractured at K=1.6MPam$^{\frac{1}{2}}$, in the transition region, $d_F \sim 100\mu m$, and the number of dislocations N is about 100. The corresponding predicted values of d_F and N are ~30μm and ~350 respectively. Exact quantitative agreement is not expected because of the severe simplifying assumptions made in the model but the order of magnitude agreement is encouraging; more recent calculations for a simple mode I geometry (Roberts, unpublished) give better agreement.

In conclusion, the observed sharp transition and the temperature at which it occurs is explained satisfactorily on the delayed nucleation model. The conditions for a sharp transition are $K_o \sim K_{Ic}$ and $K_N << K_o$. However, in order to explain the observed relation $\dot{K}/v_o(T_c)$ = constant, K_o must be independent of temperature or itself a function of $(\dot{K}/v_o)$ (see §5). Since the shape of the transition is insensitive to K_N, as long as $K_N << K_o$, K_N could have some temperature dependence.

7. A MODEL FOR NUCLEATION OF CRACK TIP SOURCES

The computations and the experiments described above show that the nature of the brittle-ductile transition in Si is sharp because no significant

dislocation generation takes place at the crack tip until crack tip sources are generated at K_o just below K_{Ic}. Once formed these sources begin to operate at K_N ($<K_o$), sending out avalanches of dislocations which produce rapid shielding. We describe here a possible mechanism for this 'delayed nucleation'. Since the precursor cracks have been introduced by indentation, there will be an associated plastic zone close to the surface. Dislocations in the plastic zone may glide to the crack tip under the influence of the crack tip stress field, which is weak initially but increases in strength as the dislocation approaches the tip. When the dislocation reaches the tip, the dislocations can cross-slip over a finite length of dislocation line to generate a dislocation source. (For more details of the cross-slip mechanism, see Hirsch *et al.*, 1989). Assuming that the cross-slip process is fast compared with the time taken by the dislocation to reach the crack tip, the value of K_o may be estimated. The stress on a dislocation a distance r from the crack tip, in mode I loading, is given by

$$\tau = \frac{Kf}{(8\pi r)^{\frac{1}{2}}} \qquad (13)$$

where f is an orientation factor. Substituting in equation (9) we find

$$\frac{dr}{dt} = \frac{-(Kf)^m}{(8\pi r)^{m/2}} v_o \qquad (14)$$

At constant strain rate $\dot{K}$ (assuming f to be constant) this can be integrated to give

$$K_o^{m+1} - K_d^{m+1} = \frac{2(m+1)(8\pi)^{m/2} r_o^{(1+m/2)}}{(m+2) f^m} \left(\frac{\dot{K}}{v_o}\right) \qquad (15)$$

where K_d is the value of K at which the dislocation begins to move, r_o is the distance travelled by the dislocation to the crack front. Since m varies only slowly over the temperature range of interest, and assuming that for a given structure K_d, r_o and f to be independent of temperature, K_o is independent of temperature and a function only of $(\dot{K}/v_o)$. Thus, for a given value of $(\dot{K}/v_o)$, K_o is constant, as assumed in the analysis of the observed strain rate dependence of T_c (see §5). This means that at T_c, assuming a constant initial dislocation structure, the dislocation will always reach the crack tip (and form a source) at the same value of the applied K ($=K_o$), independent of the loading rate. The condition for the brittle-ductile transition can now be restated, namely, that a dislocation source is formed at the crack tip just in time for the source to emit sufficient dislocations to shield the most vulnerable points on the crack front before K reaches K_{Ic}.

Equation (15) also shows that T_c depends on dislocation structure, in particular through r_o, K_d. Assuming K_o, K_d, f to be constant, $(v_o/\dot{K}) \propto r_o^{1+m/2}$, and therefore for larger r_o, v_o must be greater for a given $\dot{K}$, and this implies an increase in T_c. Since the size of the plastic zone scales with the size of the crack introduced by indentation, we expect (at constant $\dot{K}$) T_c to be larger for larger crack sizes, as observed (see Fig. 2). This size effect is expected to be larger than that depending on d_{crit} (see §6, Fig. 7).

Using equation (1), we can rewrite equation (15) in the form

$$\exp(-U/kT_c) = C\dot{K}, \text{ where} \qquad (16)$$

$$C = \frac{2(m+1)(8\pi)^{m/2} r_o^{(1+m/2)}}{(m+2) f^m A(K_o^{m+1} - K_d^{m+1})} \qquad (17)$$

The nucleation model can be tested quantitatively by comparing calculated values of C with the experimental values from the intercepts of Fig. 2. From the computer calculations in §6, $K_o \sim K_{Ic} \sim 1.17 MPam^{\frac{1}{2}}$. K_d is likely to be determined by the dislocation loop lengths in the plastic zone. Transmission electron micrographs of sections through the plastic zone suggest dislocation loop lengths (ℓ) of the order of a few microns (see Samuels and Roberts, 1989). Assuming that the critical stress for dislocation movement is $\sim \mu b/\ell$,

$$K_d \sim (8\pi r_o)^{\frac{1}{2}}/f) \mu b/\ell \qquad (18)$$

and using $f \sim \frac{1}{4}$, $\ell/b \sim 10^4$, $r_o = 13.3\mu m$, we find $K_d \sim 0.46 MPam^{\frac{1}{2}}$. With the same values of f, r_o, $K_o \sim K_{Ic}$, and with m=1.2, $A = 1.51 \times 10^{-4} ms^{-1} (Nm^{-2})^{1.2}$ for intrinsic and m=1.3, $A = 1.21 \times 10^{-7} ms^{-1} (Nm^{-2})^{1.3}$ for n-type material (see George and Champier, 1979), values of C can be calculated. These are compared with experimental values in Table 2. The agreement is very good for both types of silicon. Equation (16) can of course be used to calculate

Table 2. Calculated and experimental values of ln(C)
[Units of C are $Pa^{-1} m^{-\frac{1}{2}} s$]

	intrinsic ($2 \times 10^{13} Pcm^{-3}$)	n-type ($2 \times 10^{18} Pcm^{-3}$)
Calculated from equation (17)	-35.8	-30.2
Experimental values from figure 3(a)	-36±1	-31±1

Table 3. Calculated and observed transition temperature T_c

$r_o (\mu m)$	13.3±0.9	13.3±0.9	37.4±1.4
$\dot{K} (Pam^{\frac{1}{2}} s^{-1})$	886	1487	1487
T_c(°C)(from eqn. 16)	561±3	577	628±2
T_c(°C)(experimental)	560±5	576±5*	598±2

*(Interpolated)

T_c directly for a given $\dot{K}$. Table 3 shows predicted and observed values of T_c for the slowest strain rates for the two crack sizes used, for intrinsic Si with U=2.1ev (George and Champier, 1979). The value of K_d is assumed to be the same for both crack sizes ($K_d = 0.46 MPam^{\frac{1}{2}}$). The agreement is reasonable, particularly for the smaller crack size. For the larger crack size, T_c is predicted to increase, in qualitative accord with experiment; the numerical discrepancy may be due to a different value of K_d.

The observed lack of dislocation activity for temperatures significantly below T_c is due to the fact that K_o is very close to K_{Ic}. Taking $K_o \sim 0.95 K_{Ic}$, there is only a very small temperature range at the brittle-

ductile transition, estimated at ~2°C from equation (15), in which $0.95K_{Ic}<K_o<K_{Ic}$ and brittle fracture will occur at $K(=K_{ez})=K_{Ic}$ after significant dislocation activity. Over this range of K_o dislocations emitted by the sources will not reach the most vulnerable point on the crack front before $K=K_{Ic}$. Variation in precrack length will result in a range of values of r_o for different specimens, and therefore in a range of values of T_c. This has been estimated from the observed variation in crack length, using equation (15); the results are shown in table 3, and are seen to be of the same order as the observed values.

8. THE ROLE OF EXISTING DISLOCATIONS ON THE BDT

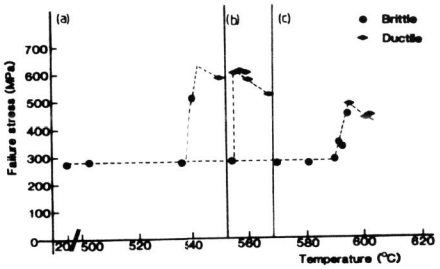

Fig. 11 Failure stress versus temperature for:
(a) 'Control' specimens. T_c=545°C;
(b) 'Abraded' specimens T_c=555°C.
(c) 'Polished' specimens. T_c=595°C;

Experiments were performed to check the proposal that the sharp BDT in Si is controlled by existing dislocations in the crystal (namely those in the plastic zone of the indentation). The top 4μm of the precracked surface of intrinsic Si specimens were polished away, thus removing much of the plastic zone at the surface. Figure 11 compares the BDT from such a specimen (curve (c)) with that of unpolished specimens (curve (a)). It is clear that T_c increases by ~55°C at $\dot{K}$~890Nm$^{3/2}$ s^{-1}. This increase confirms the importance of the existing dislocations in the plastic zone in the specimens, and this suggests that the transition is still controlled by nucleation of crack tip sources by dislocations which have not been removed by the polishing treatment. The increase in T_c then implies that existing dislocations either have a higher operating stress/smaller loop length (i.e. greater K_d) or are further away from the crack. (For further details, see Warren, 1989). The higher values of T_c found by St.John (1975) in his experiments, compared to those in the Oxford experiments, for the same strain rates (see Fig. 2), are also attributed to a smaller dislocation density/source size in St.John's experiments. In the latter's experiments the cracks were introduced in a different manner, without forming a surface plastic zone. The origin of the dislocation sources in his crystals is not known.

A further check of the model has been made by grinding the surface of the polished specimen. This should introduce dislocations at the surface, and T_c would be expected to decrease again. Figure 11(b) shows the experimental results; T_c is now 40°C lower than for the polished specimen, in agreement with the predicted trend.

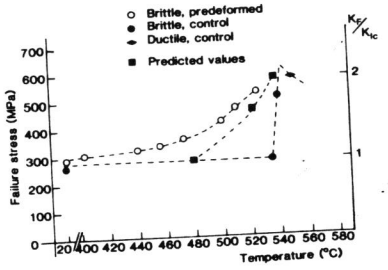

Fig.12 Failure stress versus temperature for pre-deformed specimens compared with 'normal' specimens, and a computer simulation.

The computer simulations of the emission of dislocations from the crack tip predict that a sharp transition occurs when crack tip sources are formed at K_o~K_{Ic}, which, once formed, operate at $K_N<<K_o$ (see Fig. 9). If, however, such sources already exist in the precracked specimen before the test begins, the transition should be "soft", as shown in Fig. 8. To test this prediction, standard precracked specimens of intrinsic Si were deformed at T_c to a value of K~0.9K_{Ic}, then unloaded, cooled to lower temperatures and reloaded to fracture at the new temperature. The pre-deformation should be just sufficient to nucleate crack tip sources, or to make the time needed for nucleation negligible. Figure 12 shows the results of such a set of experiments. The BDT of the pre-deformed specimens is now "soft" as predicted, and crack tip plasticity induced at lower temperatures. Figure 12 also shows for comparison a computer simulation curve for the case $K_N=0.2K_{Ic}$, for comparable strain rates. Observations of dislocation distributions on the etched surface of the cracked specimens show a progressive increase in dislocation generation with increasing temperature of testing, as expected. (For further details, see Warren, 1989).

Existing dislocation sources in the crystal may not always control the BDT. For a given ℓ they must lie within a certain distance r_o from the crack tip. It follows from equation (15) that a necessary condition is $K_d<K_{Ic}$, i.e. from equation (15),

$$r_o^{\frac{1}{2}} < (K_{Ic}\, f/(8\pi)^{\frac{1}{2}}\mu)(\ell/b) \qquad (19)$$

Thus, for example, taking f = 0.7 for silicon, if $\ell/b \sim 10^4$, r_o < 650μm. If no suitable sources are present within the appropriate radius r_o, the BDT will be controlled by other processes, e.g. the Rice-Thomson (1974) nucleation mechanism. This may be the situation in experiments on precracked thin foils of silicon by Chiao and Clarke (1987), who have reported the emission of dislocations from cracks in the absence of any existing dislocations in the crystal.

9. DISCUSSION AND CONCLUSIONS

a) The fact that in the specimens of Si which have not been pre-deformed, no dislocations are emitted from the precracks until $K>0.95K_{Ic}$, implies that

for Si there must be an energy barrier for dislocation loop nucleation by the Rice-Thomson mechanism for K values at least up to this level. This work shows that for such a material, pre-existing dislocations in the crystal can control the BDT, even if the initial dislocation density is very low. The reason is that crack-tip sources can operate at values of $K_N << K_{Ic}$, the value of K_N depending on the length of the source. Such crack-tip sources can either exist already in the specimen before the stress is applied, or they can be produced by existing dislocations in the specimen moving to the crack and transforming into sources during loading.

b) The strength and distribution of the existing dislocation sources are very important. Sources situated at or close to the crack tip are most effective in shielding (and blunting) the crack, and even a small number of such sources can produce rapid shielding along the crack front. If such sources pre-exist at or near the precrack, the BDT is soft. In Si such crack-tip sources can be produced by suitable pre-deformation at T_c, and the BDT is found to be soft as predicted. Such soft transitions are observed in b.c.c. metals containing precracks introduced by spark-machining (Hull *et al*, 1965; Liu and Bilello, 1977; Ripley, 1981). Etch pit observations on precracked single crystals of tungsten (Liu and Bilello, 1977) show a high density of dislocation etch pits near the crack front prior to loading. It is possible therefore that in these cases also the BDT is controlled by existing dislocations.

If such sources are not present, then the BDT is controlled by the time taken for nucleation of such dislocation sources by movement of existing dislocations to and interaction with the crack front. Under such conditions the BDT is sharp, an avalanche of dislocations being emitted. The source nucleation mechanism requires the presence in the specimen of dislocations which can move towards the crack at a value of $K < K_{Ic}$. If no such dislocations exist, then the BDT will be controlled by the Rice-Thomson mechanism. This may be the case in electron microscope experiments on crack propagation in thin foils, where emission of dislocations from crack tips, without the help of existing dislocations, has been observed in b.c.c. metals (Ohr, 1985) and in Si (Chiao and Clarke, 1987).

c) In the experiments on pre-cracked Si described here, no significant dislocation generation occurs during brittle crack propagation at the BDT, i.e. after the pre-crack becomes unstable. The extensive plastic zone is developed **during loading** up to the instability point, and the strain rate dependence of T_c has a simple explanation in terms of the stress and temperature dependence of the dislocation velocity in the loading part of the test. The increase in the fracture stress at the BDT is controlled by plastic relaxation during loading, and this conclusion may be generally applicable when rapid unstable cleavage fracture occurs. This point has already been stressed by others, e.g. by Liu and Bilello (1977). Different considerations must of course apply to the conditions of arrest of fast running cracks.

d) Two new mechanisms have been identified which make it possible for cleavage to occur after some crack tip plasticity. Firstly, while cleavage fracture is governed by the local stress intensity factor K_e reaching K_{Ic}, dislocation emission is controlled by a critical stress at a finite distance from the crack-tip, r_c. The crack-tip stress at r_c will not be adequately described by K_e when the emitted dislocations remain close to the crack tip. This difference can increase as more dislocations are emitted so that K_e must increase for further emission to occur, and eventually K_{Ic} is reached. This situation can arise at low temperatures when the dislocation velocity

is low, or when the emitted dislocations meet obstacles (work hardening), etc. Secondly, if shielding occurs by generation of dislocations from a finite number of sources at the crack tip, the emitted dislocations have to run sufficiently far to shield those parts of the crack away from the sources. Thus, even though crack-tip sources continue to emit dislocations, the dislocations may not be able to move fast enough, because of their internal interaction, to continue to produce adequate shielding as K increases.

e) This work shows that "warm prestressing" can have two effects. Firstly, deformation at or above T_c leads to shielding at lower temperatures by the "frozen-in" dislocations, and therefore to an increase in fracture stress in the "brittle" regime. Secondly, in cases where the (mobile) dislocation density near the crack tip is low, and the BDT is sharp, pre-deformation at T_c up to K_{Ic} generates efficient crack-tip sources; the BDT becomes soft and is shifted to lower temperatures.

f) The main parameter controlling the BDT is the dislocation velocity. Any mechanism which reduces the average velocity, e.g. radiation damage, solution or precipitation hardening, is likely to increase T_c; such mechanisms of course also increase the yield stress. The effect of dislocation density is more complex, since the distance of a source from the crack and its strength (loop length) are important, as well as the interaction of the emitted dislocations with the existing dislocations in the material. This requires further detailed consideration. Obstacles to the propagation of the plastic zone, such as grain boundaries, should lead to a back stress which reduces dislocation velocity and promotes fracture. Such effects can be taken into account in the dynamic model, but no computations have yet been carried out.

Acknowledgements

Our thanks are due to the S.E.R.C. and B.P. Venture Research Unit for financial support.

REFERENCES

Bilby, B.A., A.H. Cottrell and K.H. Swinden (1963). The spread of plastic yield from a notch. *Proc.R.Soc.Lond.* A272, 304-314.

Brede, M. and P. Haasen (1988). The brittle-to-ductile transition in silicon as a model substance. Submitted to *Acta Metall.*

Chang, S.J. and S.M. Ohr (1981). Dislocation-free zone model of fracture. *J.App.Phys.* 52, 7174-7181.

Chiao, Y.H. and D.R. Clarke (1988). Direct observation of dislocation emission from crack tips in silicon at high temperatures. Submitted to *Acta Metall.*

Cook, R.F. and B.R. Lawn (1983). A modified indentation toughness technique. *J.Am.Ceram.Soc.* 66, C 200-201.

George, A. and G. Champier (1979). Velocities of screw and 60° dislocations in n- and p-type silicon. *Phys.Stat.Sol.* 53a, 529-540.

Hirsch, P.B., S.G. Roberts and J. Samuels (1987). The dynamics of dislocation generations at crack tips and the ductile-brittle transition. *Scripta Metall.* 21, 1523-1528.

Hirsch, P.B., S.G. Roberts and J. Samuels (1988). Dislocation mobility and crack-tip plasticity at the ductile-brittle transition. *Revue Phys.Appl.* 23, 409-418.
Hirsch, P.B., S.G. Roberts and J. Samuels (1989). The brittle-to-ductile transition in silicon. II: Interpretation. *Proc.R.Soc.Lond.* in press.
Hull, D., P. Beardmore and A.P. Valintine (1965). Crack propagation in single crystals of tungsten. *Phil.Mag.* 12, 1021-1041.
Imai, M. and K. Sumino (1983). In-situ X-ray topographic study of the dislocation mobility in high-purity and impurity-doped single crystals. *Phil.Mag.* A47, 599-621.
Lakshaman, V. and J.C.M. Li (1989). Edge dislocations emitted along inclined planes from a mode I crack. Paper in preparation.
Lin, I.-H. and R. Thomson (1986). Cleavage, dislocation emission and shielding for cracks under general loading. *Acta Metall.* 34, 187-207.
Liu, J. and J.C. Bilello (1977). Effects of plastic relaxation on the semi-brittle fracture of <100> oriented tungsten single crystals. *Phil.Mag.* 35, 1453-1472.
Majumdar, B. and S.J. Burns (1981). Crack-tip shielding - an elastic theory of dislocations and dislocation arrays near a sharp crack. *Acta Metall.* 29, 579-588.
Newman, J.C. Jr. and I.S. Raju (1981). An empirical stress-intensity factor equation for the surface crack. *Eng.Frac.Mech.* 15 185-192.
Ohr, S.M. (1985). An electron microscope study of crack tip deformation and its impact on the dislocation theory of fracture. *Mat.Sci. & Eng.* 72, 1-35.
Paskin, A., B. Massoumzadeh, K. Shukla, K. Sievadzki and G.J. Dienes (1985). Effect of atomic crack tip geometry on local stresses. *Acta Metall.* 33, 1987-1996.
Rice, J. and R. Thomson (1974). Ductile versus brittle behaviour of crystals. *Phil.Mag.* 29, 73-97.
Ripley, M.I. (1981). The deformation and fracture of molybdenum and its dilute alloys. D.Phil. Thesis, University of Oxford.
Samuels, J. and S.G. Roberts (1989). The brittle-to-ductile transition in silicon. I: Experiments. *Proc.R.Soc.Lond.* in press.
Secco d'Aragona, F. (1972). Dislocation etch for (100) planes in silicon. *J.Electrochem.Soc.* 119, 948-951.
Sinclair, J.E. (1985). Slip and cleavage from blunted cracks. In: *Fundamentals of Deformation and Fracture* (B.A. Bilby, K.J. Miller and J.R. Willis, Eds.), p.628.
Sinclair, J.E. and J. Finnis (1983). Crack-tip blunting versus cleavage extension. In: *Atomistics of Fracture* (R. Latanision and J. Pickens, Eds.), pp.1047-1051. John Wiley, New York.
St.John, C. (1975). The brittle-to-ductile transition in pre-cleaved silicon single crystals. *Phil.Mag.* 32, 1193-1212.
Thomson, R. (1978). Brittle fracture in a ductile material with application to hydrogen embrittlement. *J.Mater.Sci.* 13, 128-142.
Thomson, R. (1986). Physics of fracture. In *Solid State Physics* (H. Ehrenreich & D. Turnbull, Eds.), vol. 39, pp.1-129. Academic Press, New York.
Warren, P.D. The brittle-to-ductile transition in silicon: the influence of pre-existing dislocation arrangements. *Scripta Metall.* in press.
Weertman, J. (1978). Fracture mechanics - a unified view for Griffith-Irwin-Orowan cracks. *Acta Metall.* 26, 1731-1738.